

The influences of oxygen impurity contained in nitrogen gas on the annealing of titanium nitride

Fu-Hsing Lu*, Jen-Li Lo

Department of Materials Engineering, National Chung Hsing University, 250 Kuo Kuang Road, Taichung 402, Taiwan, ROC

Received 28 March 2001; received in revised form 2 August 2001; accepted 15 August 2001

Abstract

Commercially available pure nitrogen gas often possesses a small amount of oxygen impurity that may react with many materials at high temperature. In this research the influences of the oxygen impurity contained in the nitrogen gas on the annealing of a nitride model system- titanium nitride pellets were investigated in the temperature range 400–1200 °C. Analyzing the in-situ oxygen partial pressure changes when titanium nitride samples were placed in a gas-tight furnace during annealing gives that the dissolution of oxygen in TiN is exothermic and the solubility decreases with increasing temperature. The oxidation involves simultaneously the dissolution of oxygen and the oxide scale formation. X-ray diffraction results show that TiO₂ rutile phase is present above 700 °C. Changes in the relative integrated intensity and in the morphology after annealing have also been discussed. © 2002 Elsevier Science Ltd. All rights reserved.

Keywords: Annealing; Oxidation; Oxide scale; TiN; Dissolution

1. Introduction

Commercially available pure nitrogen gas (4N–6N) usually possesses a small amount of oxygen impurity, which may react with many metals or non-oxide ceramics at high temperature. Since the oxygen incorporation may influence greatly the properties of materials, it is essential to understand the influences of the oxygen impurity when annealing such materials in nitrogen gas that is commonly used in material processing. Nevertheless, so far there is a lack of systematic research on this subject. Titanium nitride has been employed as a model nitride system in this research due to its excellent wear resistance, corrosion resistance, chemical stability, diffusion barrier property, etc. The objective of this research is to investigate how the oxygen impurity contained in the “pure” nitrogen gas affects titanium nitrides during annealing.

In the literature, it has been reported that TiN films,^{1–6} TiN powders,⁷ and TiN plates⁸ often follow a parabolic or pseudo-linear oxidation. In these cases the

dissolution of oxygen in TiN during oxidation has not been investigated. The role of oxygen in the annealing of TiN is not yet clear. Although a large amount of oxygen content up to 35 a/o has been detected in TiN films,⁹ no data are available in the literature concerning the solubility of oxygen in TiN. Since the oxygen incorporation may influence greatly the properties of TiN, it is important to further explore this subject.

In this research a self-made oxygen sensor has been used to detect the in-situ oxygen partial pressure changes in the furnace during annealing. From analyzing the changes in the oxygen partial pressure, the information concerning the dissolution of oxygen and the formation of oxide scale in TiN samples could be obtained. Pellet samples have been employed owing to the ease of sample preparation and the increase of reaction area. The weight changes after annealing will also be analyzed. The changes in the microstructure and morphology will also be discussed.

2. Experimental

The purity level of the starting TiN powders (Cerac, Inc.) is 99.5% and the mean particle size is 44 µm (325

* Corresponding author. Tel.: +886-4-2285-1455; fax: +886-4-2285-7017.

E-mail address: fhlu@dragon.nchu.edu.tw (F.-H. Lu).

mesh). The composition of the powders is about $\text{TiN}_{0.92}$ which is nitrogen deficient but close to a stoichiometry composition. The phase was identified to be a rock-salt structure (JCPDS 38-1420) and the lattice parameter was determined to be 0.424 nm. The powders about 1.3 g for each sample were cold pressed into the disks with the size of about 17 mm in diameter and 1.9 mm in thickness. The green density of the TiN pellets was about 58% of the theoretical density (5.213 g/cm^3).¹⁰

The purity level of the commercial available nitrogen gas used in the annealing is 99.999%. The nitrogen was firstly flowed into a gas-tight tube furnace at different temperatures and in-situ monitored by a self-made oxygen sensor (15 mol%-CaO doped ZrO_2). The oxygen impurity level in the nitrogen was then determined as a reference state. The flow rate of nitrogen was controlled at 200 sccm by a UNIT UFC 8100 mass flow meter. After that, the TiN pellets were annealed separately in the furnace at different temperatures ranging from 400 to 1200 °C for a soaking time of 1 h. The ramping rate was about 5 °C/min. The temperatures were monitored by a R-type thermocouple, which was placed closely to the oxygen sensor. The changes in the oxygen partial pressures were also in-situ determined by the oxygen sensor. After annealing, the weight changes of the samples were also measured.

The phase changes were determined by X-ray diffraction (MacScience MXP3, X-ray source: $\lambda_{\text{Cu}, \text{K}\alpha 1} = 1.5406 \text{ \AA}$). Some of the samples were also ground layer by layer by SiC sandpapers. A Mitutoyo depth indicator with the resolution of 1 μm was used to determine the layer thickness being ground away from the sample surface. X-ray diffraction was also used to examine the structure changes in the interior of the samples after annealing. The morphology of the samples after annealing was examined by a Jeol JSM-5400 SEM (accelerating voltage 20 kV).

3. Results and discussion

3.1. Oxygen partial pressure changes

Firstly it is important to know the oxygen impurity level of the nitrogen gas used in the annealing as a reference. When nitrogen was flowed into the tube furnace without placing any samples (blank test), the measured oxygen partial pressures at different temperatures starting from 600 °C were mostly of the order of 10^{-5} atm (corresponding to 10 ppm impurity) that is reasonable considering oxygen is the major impurity in the nitrogen. Only at 1200 °C the value of the oxygen partial pressure was a little bit higher and reached about 10^{-4} atm. The p_{O_2} (solid line)–temperature (dashed line) versus time curves for the blank test are shown in Fig. 1. As given in the figure, the oxygen sensor would detect

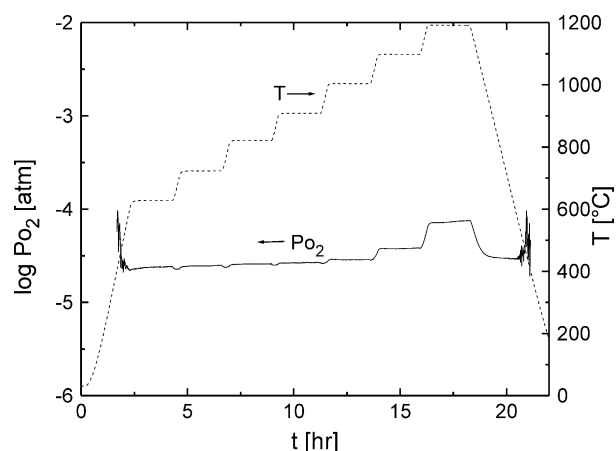


Fig. 1. The measured p_{O_2} (solid line)–temperature (dashed line) versus time curves for the blank test where nitrogen was flowed into the gas-tight furnace without any tested sample.

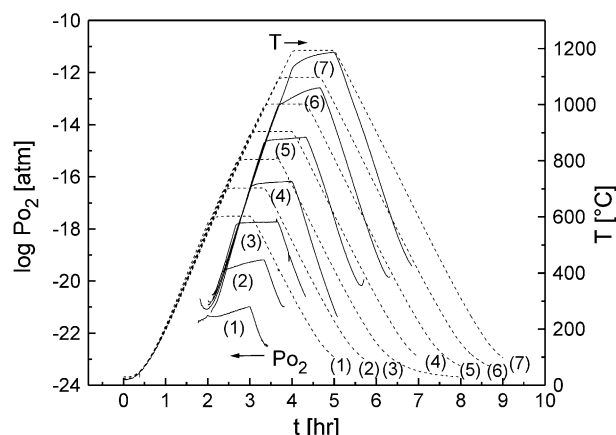


Fig. 2. The measured p_{O_2} (solid lines)–temperature (dashed lines) versus time curves for the case where TiN pellets were annealed in the nitrogen at various soaking temperatures: (1) 600 °C, (2) 700 °C, (3) 800 °C, (4) 900 °C, (5) 1000 °C, (6) 1100 °C and (7) 1200 °C.

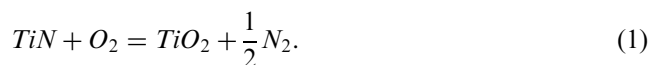
mostly noises below 600 °C but could provide meaning data above that temperature, hence only the data above 600 °C were used in the following analyses.

When each TiN pellet was placed in the furnace and annealed in the same atmosphere, a dramatic decrease of p_{O_2} was observed for all the temperature ranges we preformed. Fig. 2 gives the p_{O_2} (solid lines)–temperature (dashed lines) versus time curves for the TiN samples annealed in the nitrogen at various soaking temperatures: (1) 600 °C, (2) 700 °C, (3) 800 °C, (4) 900 °C, (5) 1000 °C, (6) 1100 °C and (7) 1200 °C. As shown in the figure, the oxygen partial pressure dropped dramatically and remained almost constant as low as 10^{-21} atm at 600 °C, which is about 16 orders of magnitude lower than the value obtained from the blank test. Annealing the samples at high temperature like 1200 °C still resulted in a 6 orders of magnitude decrease, i.e. 10^{-11} atm.

The trend of all obtained p_{O_2} curves is similar. A typical p_{O_2} -temperature versus time curve is enlarged for 900 °C in Fig. 3 to examine closely the meaning of the trend. It is worth noting that the measured oxygen partial pressure is reversible when ramping up and down. Moreover, the p_{O_2} -values increased with increasing temperature and remained almost constant when temperatures were kept constant. It is shown in the figure that when temperature reached 600 °C during ramping either up or down, the values of oxygen partial pressures were about the same at 10^{-21} atm that is almost the same as that described earlier at the soaking temperature of 600 °C. The obtained p_{O_2} -values were also plotted in logarithm against those soaking temperatures (see Fig. 4). As shown in the figure, $\log p_{O_2}$ -values decreased linearly with $1/T$, which will be discussed below.

The measured p_{O_2} represents the oxygen content remaining in the furnace when part of the oxygen impurities in the flowing nitrogen gas react with the TiN samples and the reaction reaches a steady state. The dramatic decrease in the measured p_{O_2} with TiN samples in the furnace may primarily attribute to either the formation of the oxide scale or the dissolution of oxygen into TiN since both reactions require the supply of oxygen from the flowing gas.

Firstly assume the measured p_{O_2} decrease is mainly due to the formation of the oxide scale and consider only TiO_2 phase is formed during the oxidation, the oxidation reaction of TiN can be formulated as:



The free energy change (ΔG , in kJ/mol) for the oxidation of TiN films in the temperature range 298–1943 K, which has been discussed in our previous paper,¹¹ can be written as

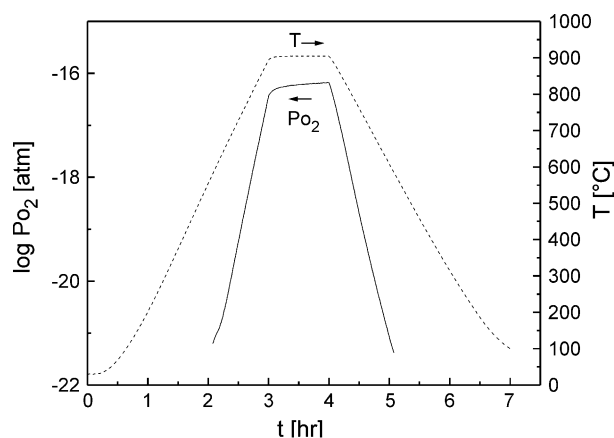


Fig. 3. Enlarged typical p_{O_2} -temperature versus time curve for Fig. 2.

$$\begin{aligned} \Delta G &= RT \left[\ln \left(\frac{p_{N_2}^{1/2}}{p_{O_2}} \right) - \ln \left(\frac{p_{N_2}^{1/2}}{p_{O_2}} \right)_{eq} \right] \\ &= 8.314 \times 10^{-3} T \times \ln \left(\frac{p_{N_2}^{1/2}}{p_{O_2}} \right) - 604.7 + 0.084 T \end{aligned} \quad (2)$$

where T is in the unit of K and $(p_{N_2}^{1/2}/p_{O_2})_{eq}$ represents a fixed gas partial pressure ratio at which TiN is in thermodynamic equilibrium with TiO_2 . When TiN is annealed in nitrogen $[(p_{N_2}^{1/2}/p_{O_2}) \sim 10^5]$, $\Delta G < 0$ for all the temperature range used in this research since TiO_2 is much more stable than TiN even in the nitrogen. The oxidation of TiN would mainly follow either a parabolic rate law or a linear rate law depending on the rate-limiting mechanism.^{1–8} Nevertheless the oxidation rate should increase with temperature,¹² which indicates that the observed p_{O_2} (oxygen content remaining in the annealing environment) should decrease with temperature. Apparently it is not the case here; hence the dramatic decrease of p_{O_2} cannot be mainly due to the formation of the oxide scale on TiN.

Another possibility for the dramatic decrease of the observed p_{O_2} is primarily due to the dissolution of oxygen into TiN samples during annealing although the oxide scale would be simultaneously formed on the sample surface. In this case the oxide should be porous

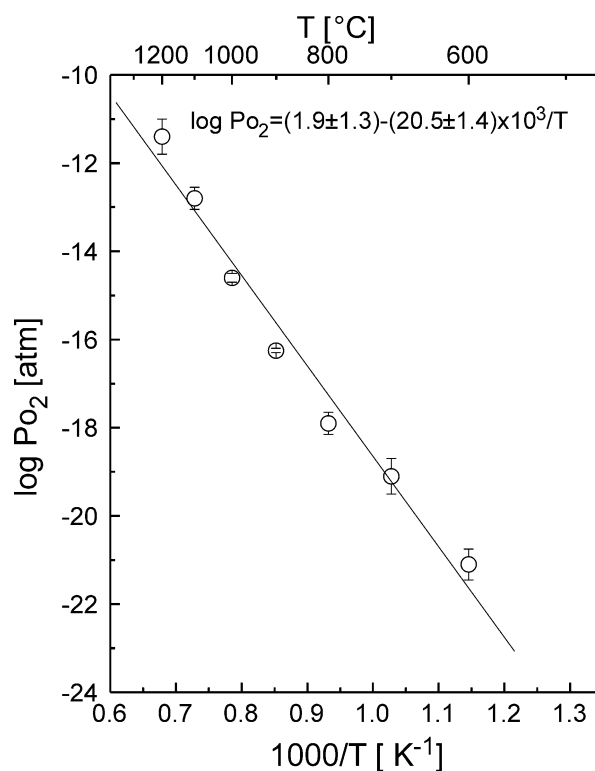


Fig. 4. The logarithm of p_{O_2} -values at soaking temperatures deduced from Fig. 2 decrease linearly with $1/T$.

enough to allow the rapid penetration of oxygen. The dissolution reaction can be formulated as



The equilibrium constant k for the dissolution reaction could be written as

$$k = \frac{(\gamma_O \times x_O)^2}{p_{O_2}} \quad (4)$$

where γ_O is the activity coefficient and x_O is the mole fraction (solubility) of oxygen in TiN. The mole fraction of oxygen dissolved into TiN can then be rewritten as the following, which is known as Sieverts's law.¹³

$$\begin{aligned} x_O &= \frac{\sqrt{k}}{\gamma_O} \times \sqrt{p_{O_2}} = k' \times \sqrt{p_{O_2}} \\ &= c \times \exp\left(\frac{b}{T}\right) \times \sqrt{p_{O_2}} \end{aligned} \quad (5)$$

where k' often is exponential with temperature and can then be expressed as $c \cdot \exp(b/T)$ where b and c are constants.¹⁴ If the constant b is negative, then the dissolution is an endothermic reaction and the solubility would increase with increasing temperature for a constant applied pressure, and vice versa. Considering our case for the oxygen dissolution in TiN, the reaction could only possibly be exothermic (b is positive) and the oxygen solubility would decrease with increasing temperature. Hence, the observed p_{O_2} values, representing the remaining oxygen in the gas, should increase with increasing temperature, as observed in this research. Apparently, the oxide scale formed at high temperatures, which will be discussed later in the XRD section, is not dense enough to prohibit the rapid penetration of oxygen hence the oxygen can diffuse rapidly through the oxide scale and then dissolve into the bulk TiN region. That's why the p_{O_2} -values still decrease when cooling down since the solubility of oxygen in TiN increases with decreasing temperature.

Consider a portion of the original flowing nitrogen as a closed system, the oxygen content ($10 \text{ ppm} = 10^{-5}$) in the flowing nitrogen must be equal to the oxygen dissolved into TiN (mole fraction, x_O) plus the oxygen content remaining in the nitrogen (observed p_{O_2} values) due to the conservation of matter. Hence Eq. (5) could be rewritten as

$$x_O = 10^{-5} - p_{O_2} = c \times \exp\left(\frac{b}{T}\right) \times \sqrt{p_{O_2}} \quad (6)$$

$$\frac{10^{-5}}{\sqrt{p_{O_2}}} - \sqrt{p_{O_2}} = c \times \exp\left(\frac{b}{T}\right) \quad (7)$$

Since the values of measured p_{O_2} (in the unit of atm), function of temperature, are much lower than 10^{-5} atm, the second p_{O_2} -term can be neglected. Rewriting Eq. (7) gives

$$\begin{aligned} \log p_{O_2}(T) &= c' - \frac{b'}{T} \\ &= (-10 - 2 \times \log c) - \frac{b}{1.151 \times T} \end{aligned} \quad (8)$$

where p_{O_2} is in the unit of atm and T is in K. Fitting the data shown in Fig. 4 with the above equation gives $c' = 1.9 \pm 1.3$ and $b' = (20.5 \pm 1.4) \times 10^3$ [K]. Since b ($= 1.151 \times b'$) is positive, it is confirmed that the dissolution of oxygen into TiN is exothermic and then the oxygen solubility decreases with increasing temperature. That's why the measured p_{O_2} values in the furnace increase with increasing temperature.

Rearranging Eqs. (6)–(8) gives the solubility of oxygen in TiN when annealing in nitrogen, x_O , as

$$\begin{aligned} \log x_O &= \log c + \frac{b}{2.303 \times T} + \frac{1}{2} \times \log p_{O_2} \\ &= -(6.0 \pm 0.6) + \frac{(10.3 \pm 0.7) \times 10^3}{T} + \frac{1}{2} \\ &\quad \times \log p_{O_2} \end{aligned} \quad (9)$$

where T (K) is the annealing temperature, p_{O_2} (atm) is the measured oxygen partial pressure in the furnace. The model developed here can also be used to determine the solubility of oxygen in the nitride when annealing is performed in other atmospheres.

To confirm the validity of the model, another experiment with a considerably small amount of TiN powders (0.02 g \sim 1.5 wt.% of previous samples) for a faster reaction was performed. The small amount of TiN powders was annealed in nitrogen with the same conditions as used for the previous TiN samples. A high soaking temperature 1200° was selected to increase the reaction rate. The resulted p_{O_2} atm (solid line)—temperature (dashed line) versus time curves is given in Fig. 5. The obtained p_{O_2} can be divided into two regions, I and II, as denoted in the figure. Region I represents the dissolution of oxygen into TiN as discussed earlier and Region II corresponds to the occurrence of complete oxidation of TiN. A sharp increase of p_{O_2} can be observed between the two regions. As we discussed earlier that oxygen would continually penetrate rapidly through the formed oxide and dissolve into TiN; hence the solubility would decrease with increasing temperature. As long as the dissolution proceeds, the low p_{O_2} values should be expected. When TiN is completely oxidized into TiO_2 , the dissolution of oxygen would end and the p_{O_2} value would increase drastically back to the reference level as observed from the blank

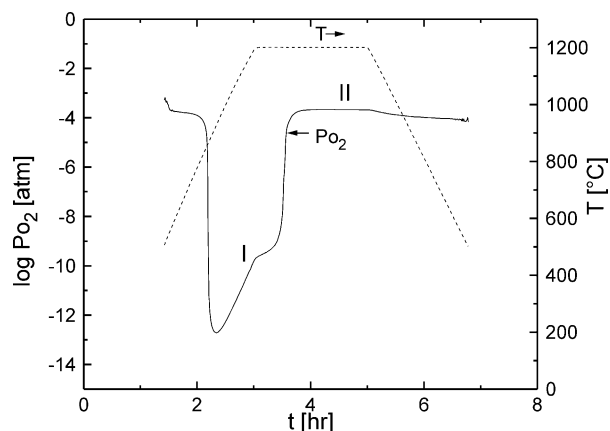


Fig. 5. The p_{O_2} (solid line)–temperature (dashed line) versus time curve for a small amount of TiN powders annealed in nitrogen. A sharp increase of p_{O_2} represents that TiN was completely oxidized into TiO_2 .

test. When cooling down the p_{O_2} value remained at the reference level and would not decrease again, which is different from what we observed in all previous samples since the dissolution of oxygen could no longer proceed.

When annealing in any other controlled atmosphere besides nitrogen, the mole fraction of oxygen dissolved into TiN can be generalized as

$$x_O = p_{O_2(in)} - p_{O_2(out)} = C \times \exp\left(\frac{B}{T}\right) \times \sqrt{p_{O_2(out)}} \quad (10)$$

p_{O_2} represents the oxygen content in the supplied gas flowing into the furnace. Its value can be easily obtained by the supplier or measured by an oxygen sensor from the blank test as mentioned earlier. $p_{O_2(out)}$ (atm), can be measured by an oxygen sensor in the furnace, represents the oxygen content remaining in the gas after a certain fraction of oxygen dissolves into the samples. C and B , temperature-independent constants, can be obtained by analyzing the measured oxygen partial pressures at various temperatures as described above for the case of annealing in nitrogen. It is worth noting that the above model can also be applied to other non-oxide material systems, which can dissolve oxygen to a certain extent.

3.2. Weight changes

After annealing, the weight of the TiN samples increases about exponentially with temperature varying from 400 to 1200 °C for a soaking time of 1 h as given in Fig. 6. Nevertheless the weight increase would only reach 2.93 wt.% at as high as 1200 °C, which is much lower than 29.1 wt.% when TiN would be completely oxidized to TiO_2 without any weight loss. That means only about 10% of TiN samples were oxidized at 1200 °C during 1 h deposition. In a separate experiment where a very small amount of TiN powders were used as

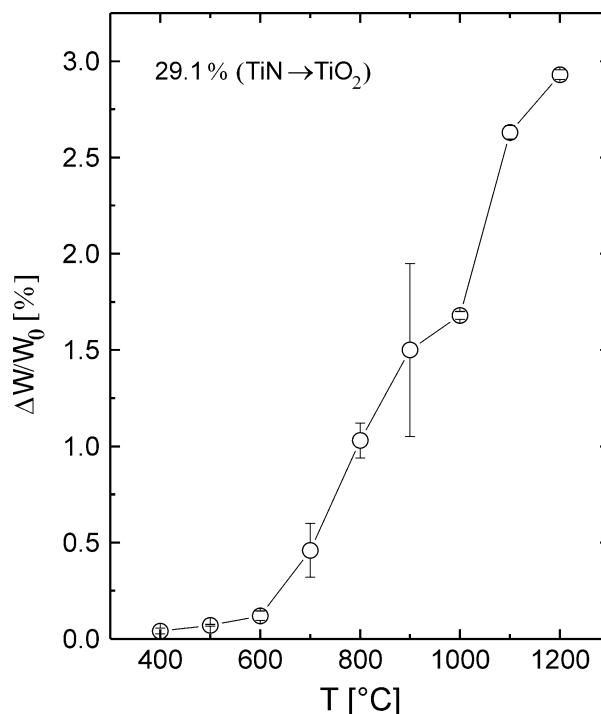


Fig. 6. The weight change of the TiN pellets after annealing in nitrogen increases about exponentially with temperature varying from 400 to 1200 °C.

mentioned earlier, the weight increase after annealing at 1200 °C was about $30 \pm 2\%$, which indicates that a complete oxidation would only occur for such a small amount of sample even at 1200 °C.

From the analyses of the measured oxygen partial pressures it is known that the solubility of oxygen in TiN is too small to be measurable in the weight changes. Hence the weight changes of the samples are mainly due to the oxide scale formation on TiN.

3.3. X-ray diffraction results

The X-ray diffraction results after annealing in nitrogen over a temperature range 500–1200 °C are given in Fig. 7. From the diffraction results, it is shown that only TiN diffraction peaks were detected below 600 °C and rutile TiO_2 appeared above 700 °C. Fig. 8 shows the relative intensity (integrated intensity) of TiN and TiO_2 , which were calculated from integrating the peak area in Fig. 7. It is clearly shown that the relative intensity of TiO_2 increased rapidly with temperature from 600 to 1100 °C and almost all the surface of the samples were oxidized above 1100 °C. Although at 1200 °C the TiN phase totally disappeared in the XRD spectra, most of the bulk region of samples still remained as TiN as discussed earlier concerning the weight changes. It is worth noting that the trend of the relative intensity of TiO_2 with temperature is quite similar to that of the weight increase. This is also another indication that the oxide

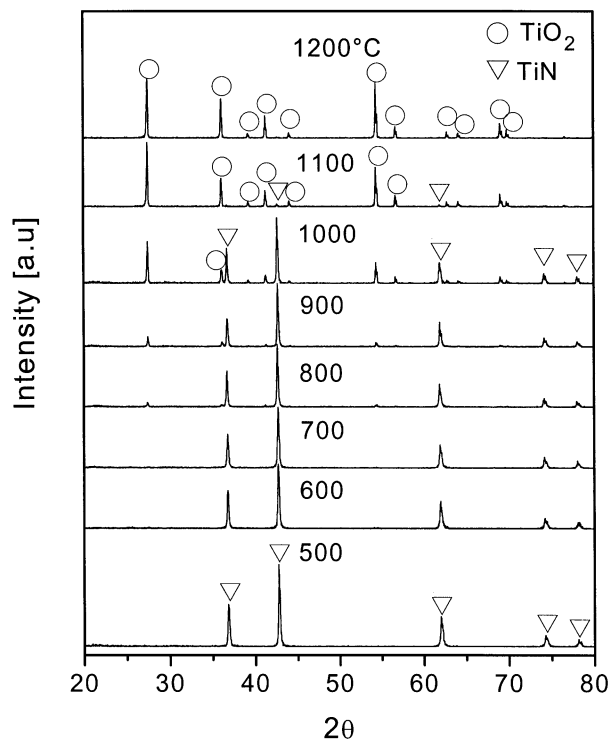


Fig. 7. X-ray diffraction results of TiN pellets annealed in nitrogen in the temperature range 500–1200 °C. Rutile TiO_2 occurred at 700 °C.

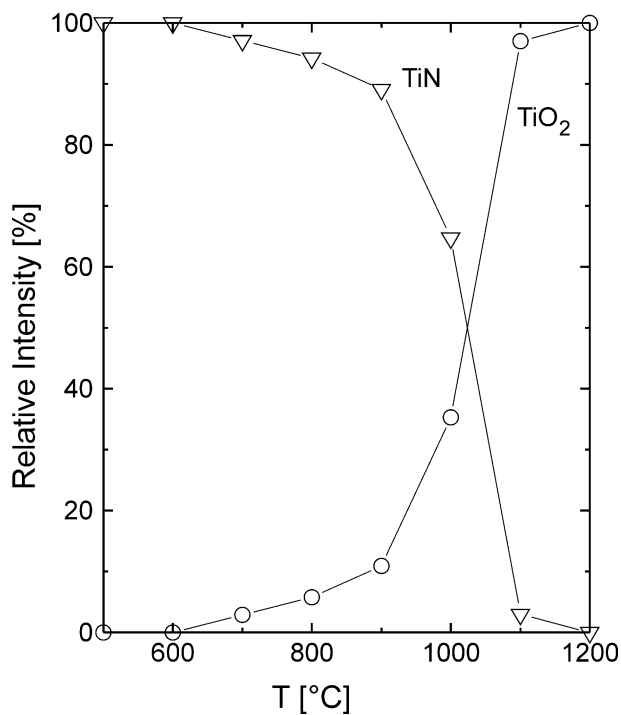


Fig. 8. The relative XRD peak intensity (integrated intensity) of TiN and TiO_2 at 500–1200 °C.

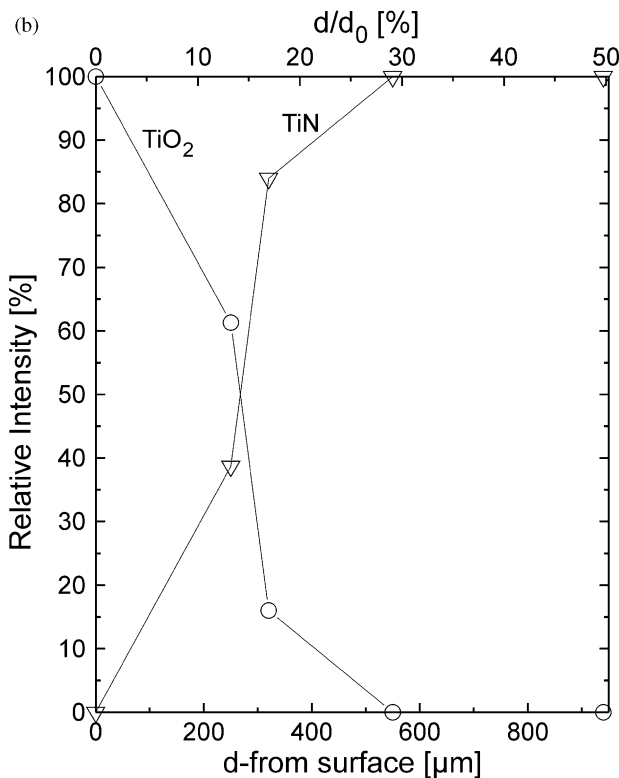
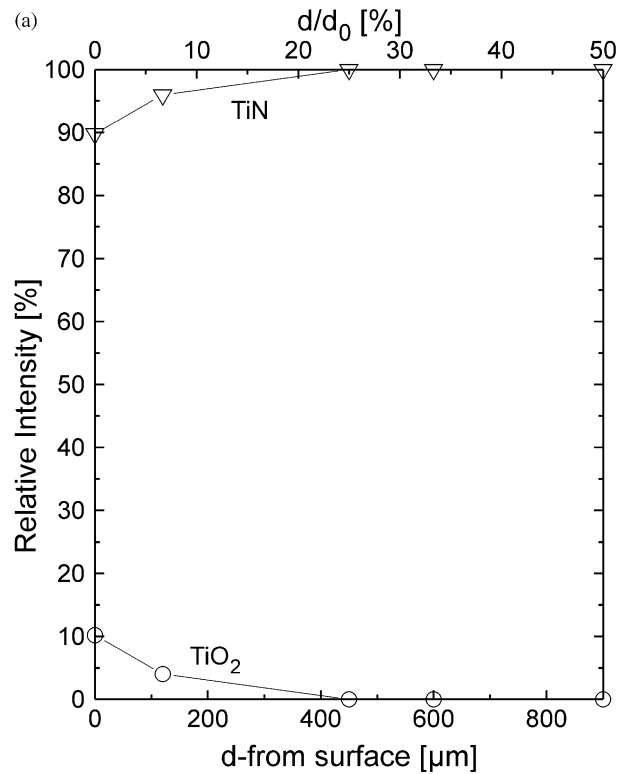


Fig. 9. The relative XRD peak intensity of TiN and TiO_2 determined at different depth of the disk samples after annealing at (a) 900 °C and (b) 1200 °C (d , depth of the layer being ground away from the sample surface; d_0 , the thickness before grinding).

scale formation is responsible for the weight increase after annealing. Some of the annealed TiN pellets were mechanically ground layer by layer from the surface and were examined by XRD to investigate the microstructural changes in the inner region of the samples. As shown in Fig. 9(a) only a small percentage of the sample surface was oxidized at 900 °C and the sample surface was totally covered by TiO₂ at 1200 °C as given in Fig. 9(b).

As discussed earlier, the oxidation of TiN involves both the TiO₂ oxide scale formation and the dissolution of oxygen into TiN. If the dissolution of oxygen into TiN is sufficiently large to cause the change of the lattice constant, the shift of the TiN diffraction angles should be observed. The lattice parameters of all the annealed samples were calculated by extrapolating the data against both $\cos^2\theta$ and $1/2(\cos^2\theta/\theta + \cos^2\theta/\sin\theta)$ (Nelson–Riley function).¹⁵ From the calculated results lattice parameters remain almost unchanged for the annealing temperatures performed. Hence, it is known that the dissolution of oxygen is too small to cause the change in the lattice parameter, which is consistent with the solubility data obtained from analyzing the mea-

sured p_{O_2} values as discussed before. From the measured p_{O_2} values, weight changes, and the XRD results, it can be concluded that the TiO₂ oxide scale formation predominates at high temperature and the dissolution of oxygen in TiN predominates at low temperature.

3.4. Morphology changes

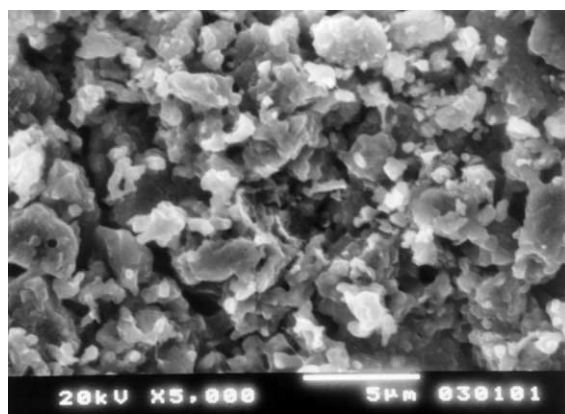
The surface morphology of TiN pellets after annealing was examined by SEM. After annealing at 1000 °C, the surface of the pellets still remained porous and the grains were rather smooth as shown in Fig. 10(a). Meanwhile the surface morphology changed drastically after annealing at 1100 °C. A rather compact layer with faceted TiO₂ grains developed as given in Fig. 10(b). As reported in Ref. 8, the morphology is closely related to the oxidation kinetics. Comparing to the previous XRD results, only a small portion of the surface region consisted of rutile TiO₂ (1000 °C) while most of the surface was covered by the oxide (1100 °C) as indicated by the relative integrated intensity.

In an ongoing research, the reactions of nitrogen with titanium metal were also investigated. The influences of the oxygen impurity contained in the nitrogen on the reaction are much more complicated since the nitridation (TiN_x, $x = 0.3, 0.5$, and 1) as well as the oxidation should all be considered. Nevertheless using similar analyses developed here would help understanding the role of the oxygen in the reactions.

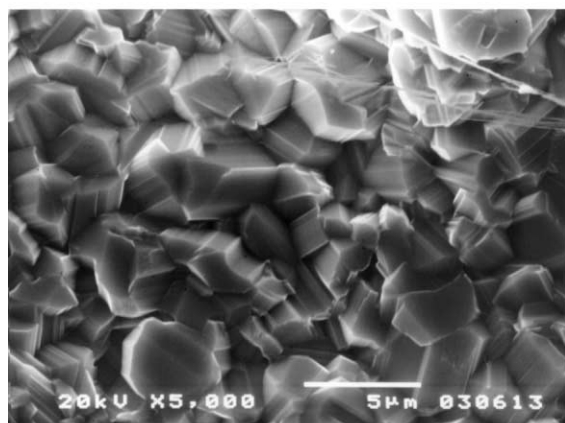
4. Conclusions

The influences of the oxygen impurity contained in commercially available nitrogen gas on the annealing of titanium nitride pellets were investigated over a temperature range 400–1200 °C by analyzing oxygen partial pressures changes, weight changes, X-ray diffraction results, and morphology changes. The oxidation of TiN involves simultaneously the oxide scale formation as well as the dissolution of oxygen into TiN. Compared to blank tests, the dramatic decrease of oxygen partial pressures when placing TiN samples in the nitrogen-flowed furnace is mainly due to the dissolution of oxygen into TiN. Analyzing the oxygen partial changes at various temperatures gives that the dissolution of oxygen into TiN is exothermic and the oxygen solubility decreases with increasing temperature.

The weight increase of the samples after annealing could primarily attribute to the oxide formation. X-ray diffraction results show that TiO₂ rutile phase is present above 700 °C. The dissolution of oxygen into TiN is too small to cause the change in the lattice parameter. Combining measured p_{O_2} values, weight changes, and XRD results gives that the TiO₂ scale formation predominates at high temperature and the dissolution of



(a)



(b)

Fig. 10. The surface morphology after annealing at (a) 1000 °C and (b) 1100 °C. Faceted rutile TiO₂ grains appeared at 1100 °C.

oxygen into TiN predominates at low temperature. Faceted rutile TiO₂ grains would appear on the surface of the TiN pellets above 1100 °C.

Acknowledgements

This work is partially supported by the National Science Council of ROC under grant No. NSC86-2216-E-005-004.

References

1. Ichimura, H. and Kawana, A., High-temperature oxidation of ion-plated TiN and TiAlN films. *J. Mater. Res.*, 1993, **8**, 1093–1100.
2. Wittmer, M., Noser, J. and Melchior, H., Oxidation kinetics of TiN thin films. *J. Appl. Phys.*, 1981, **52**, 6659–6664.
3. Sigurd, D., Suni, I., Wieluński, L., Nicolet, M.-A. and Seefeld, H., Thermal oxidation of sputtered TiN diffusion barriers. *Solar Cells*, 1981–1982, **5**, 81–86.
4. Suni, I., Sigurd, D., Ho, K. T. and Nicolet, M.-A., Thermal oxidation of reactively sputtered titanium nitride and hafnium nitride films. *J. Electrochem. Soc.*, 1983, **130**, 1210–1214.
5. Tompkins, H. G., Oxidation of titanium nitride in room air and in dry O₂. *J. Appl. Phys.*, 1991, **70**, 3876–3880.
6. Münster, A. and Schlamp, G., Über die oxidation der titannitrids II Der mechanismus der oxidation. *Z. Phys. Chem.*, 1957, **13**, 76–94.
7. Bellosi, A., Tampieri, A. and Liu, Y.-Z., Oxidation behavior of electroconductive Si₃N₄-TiN composites. *Mater. Sci Eng. A.*, 1990, **127**, 115–122.
8. Desmaison, J., Lefort, P. and Billy, M., Oxidation of mechanism of titanium nitride in oxygen. *Oxid. Met.*, 1979, **13**, 505–517.
9. Carson, R. T., Givens, J. H., Savage, H. S., Lee, Y. W. and Rigsbee, J. M., Effects of oxygen on the electrical and electrochemical properties of ion-plated titanium nitride. *Mater. Lett.*, 1992, **14**, 313–317.
10. Kroschwitz, J. I. and Grant, M. H. (Eds.), Encyclopedia of Chemical Technology, Vol. 24, Titanium Compounds. John Wiley and Sons, New York, 1997 pp. 231.
11. Lu, F.-H., Feng, S.-P., Chen, H.-Y. and Li, J.-K., The degradation of TiN films on Cu substrates at high temperature under controlled atmosphere. *Thin Solid Films*, 2000, **375**, 123–127.
12. Kofstad, P., *High Temperature Corrosion*. Elsevier Applied Science, London, 1988 pp. 15–25.
13. Sieverts, A. and Hagenacker, J., Über die löslichkeit von wasserstoff und sauerstoff in festem und geschmolzenem silber. *Z. Phys. Chem.*, 1907, **68**, 115.
14. Smith, D. P., Carney, D. J., Eastwood, L. W. and Sims, C. E., *Gases in Metals*. ASM, Cleveland, 1953 pp. 1–20.
15. Cullity, B. D., *Elements of X-ray Diffraction*, 2nd edn. Addison-Wesley, Massachusetts, 1978 pp. 355–358.